DFT Study of Solvent Coordination Effects on Titanium-Based Epoxidation Catalysts. Part One: Formation of the Titanium Hydroperoxo Intermediate

Robert R. Sever and Thatcher W. Root*

Department of Chemical Engineering, University of Wisconsin-Madison, 1415 Engineering Drive, Madison, Wisconsin 53706

Received: May 2, 2002; In Final Form: February 3, 2003

Density functional theory has been used to study the effects of solvent coordination on the structure and formation of the titanium hydroperoxo species believed to be the active intermediate in oxidation reactions with Ti(IV)−H_2O_2 catalytic systems. Titanium hydroperoxo intermediates possessing a variety of coordination environments have been modeled with unconstrained single coordination sphere clusters using a B3LYP/ECP methodology. Titanium hydroperoxo intermediates bearing one or two solvent ligands may assume several degenerate structures with the hydroperoxo moiety coordinated to titanium in a monodentate or bidentate manner. Hydrogen bonding of the hydroperoxo moiety with a protic solvent ligand via a monodentate five-membered ring structure does not confer any significant additional stabilization to the titanium hydroperoxo intermediate. The presence of a single solvent ligand on the titanium center lowers the Gibbs free energy of activation for the formation of titanium hydroperoxo intermediates by 4−8.5 kcal/mol. Hydrogen-bonded protic molecules can facilitate proton transfer from a hydrogen peroxide ligand on titanium and thereby lower the Gibbs activation barrier for intermediate formation by 5−6 kcal/mol. NBO analysis provides an enriched understanding of how solvent ligands alter structural and electronic properties and reduce activation barriers. Consideration of thermodynamic and kinetic results indicates that the most abundant titanium hydroperoxo intermediates formed under liquid-phase reaction conditions will most likely possess a single solvent ligand on titanium and possibly a hydrogen-bonded protic solvent molecule.

Introduction

Over the past two decades, heterogeneous titanium(IV)-based catalysts have received much attention for their potential to perform industrially important oxidation reactions with environmentally benign hydrogen peroxide as oxidant. In particular, the heterogeneous Ti(IV)−H_2O_2 system provides an attractive alternative for the manufacture of epoxides from olefins compared to existing stoichiometric or homogeneously catalyzed processes. Highly active and selective olefin epoxidation catalysts can be produced by atomically dispersing titanium in a silica matrix,[1−3] isomorphously substituting titanium for silicon in molecular sieve frameworks,[4−6] or grafting isolated titanium species to the surface of silica,[7−10] mesoporous molecular sieves,[11,12] or layered aluminosilicates.[13]

It has been established experimentally that the titanium active sites in these epoxidation catalysts are atomically isolated from one another and tetrahedrally coordinated under vacuum conditions.[5−6,11,14−19] The titanium atoms likely possess two, three, or four Ti−O−Si bonds to the siliceous framework or support, with the remaining tetrahedral titanium valencies occupied by hydroxyl groups (or possibly alkoxy groups in the case of Ti−O−Si solvolysis by organic solvents).[6,18−21] A DFT study by Sinclair and Catlow[22] has demonstrated that the creation of short-lived titanyl (Ti═O) species is possible in the presence of protic solvents; however, diffuse reflectance UV−vis spectra for these catalysts do not contain the characteristic titanyl group absorbance.[23] In the presence of small donor molecules, such as water, methanol, or ammonia, the titanium active site readily expands its coordination sphere to include one or two ligands.[5−6,15,16,18,19,23−24]

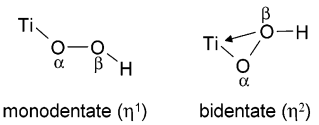

Figure 1. Possible geometries for the hydroperoxo moiety in the titanium hydroperoxo intermediate. (Arrow represents coordinative interaction with titanium.).

Addition of hydrogen peroxide to the titanosilicate catalyst yields the active oxygen-donating intermediate for epoxidation reactions. It is generally agreed that the active intermediate is a titanium hydroperoxo species (TiOOH) as opposed to a titanium peroxo species (TiOO).[25−29] The structure of this titanium hydroperoxo intermediate remains uncertain. The hydroperoxo oxygens may coordinate the titanium center in a monodentate (η^1) or bidentate (η^2) manner (Figure 1). Computational studies of titanium hydroperoxo species in the absence of solvent coordination typically show bidentate coordination for the hydroperoxo group.[30−32] Yudanov et al.[31] have reported that the hydroperoxo group in a $Ti(OH)_3(OOH)$ cluster remains bidentate upon addition of a single ammonia ligand to the titanium center. Tozzola et al.[28] found monodentate coordination for the same titanium cluster model possessing two water ligands. Recently, Sankar et al.[33] have used in situ X-ray absorption spectroscopy (XAS) in conjunction with DFT calculations to characterize the local geometry of the titanium center in Ti-grafted MCM-41 catalysts after reaction with aqueous *t*-butyl hydroperoxide. Their XANES measurements indicated that the titanium center most likely possesses octa-

* To whom correspondence should be addressed. E-mail: thatcher@engr.wisc.edu.

10.1021/jp026056s CCC: $25.00
Published on Web 03/26/2003

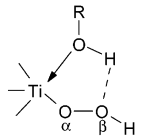

Figure 2. Schematic representation of the hydrogen-bonded five-membered ring titanium hydroperoxo intermediate proposed by Clerici and co-workers.[25,26] (Dashed line indicates hydrogen-bonding interaction.).

hedral coordination; their EXAFS and DFT results supported the formation of either a bidentate titanium hydroperoxo species with a single water ligand on titanium or a monodentate species bearing two water ligands.[33−35]

Experiments have shown that the identity of the solvent can have a pronounced effect on the activity and selectivity of titanium-based catalysts in liquid-phase epoxidation reactions.[3,26,36−42] The nature of these solvent effects is complicated due to their dependence on catalyst properties and reaction conditions, and their origin currently remains unclear. In the case of hydrophobic titanium-based catalysts, olefin epoxidation rates are generally higher in protic solvents (e.g., methanol or ethanol) than in aprotic solvents (e.g., acetonitrile or acetone).[26,36−40] To explain this trend, Clerici and co-workers[25,26] proposed the existence of a five-membered ring titanium hydroperoxo intermediate in which a protic solvent ligand on the titanium center donates a hydrogen bond to the distal oxygen of the hydroperoxo moiety (Figure 2). According to this proposal, hydrogen bonding in the five-membered ring enhances epoxidation reaction rates by either stabilizing the formation of the titanium hydroperoxo intermediate or increasing its electrophilicity. Few computational studies of the relative stability of the proposed five-membered ring intermediate have been reported.[34,35,43,44] Vayssilov and van Santen[43] determined that the dissociative adsorption of hydrogen peroxide on an unconstrained $Ti(OSiH_3)_4$ cluster to form a five-membered ring titanium hydroperoxo intermediate with a coadsorbed methanol or water ligand was highly endothermic at 21.7 or 30.8 kcal/mol, respectively. Barker et al.,[34,35] on the other hand, calculated that formation of a monodentate five-membered ring $Ti(OSiH_3)_3(OOH)\cdot H_2O$ cluster is exothermic by 9.9 kcal/mol and that the monodentate intermediate is only 0.6 kcal/mol less stable than its bidentate counterpart. No comparisons of the relative reactivities of monodentate cyclic intermediates and bidentate intermediates in the olefin epoxidation reaction have been reported. Understanding of the cyclic intermediate's possible role in the epoxidation mechanism remains limited.

Barker et al.[34] and Munakata et al.[45] have performed DFT studies of the formation mechanisms of titanium hydroperoxo intermediates using constrained cluster models in the absence of solvent coordination. Barker et al.[34] examined the transfer of a proton from a hydrogen peroxide ligand on titanium to the hydroxyl group oxygen in a $Ti(OSiH_3)_3(OH)$ cluster. They calculated separate reaction pathways for the formation of a monodentate and a bidentate $Ti(OSiH_3)_3(OOH)\cdot H_2O$ intermediate, finding activation barriers of 9.1 and 11.0 kcal/mol, respectively. Munakata et al.[45] calculated an activation barrier of 16.5 kcal/mol for proton transfer from a hydrogen peroxide ligand to a framework oxygen in a $Ti[OSi(OH)_3]_4$ cluster model.

Considering the strong influence of solvents on the performance of titanium-based epoxidation catalysts observed experimentally, it is clear that the structures and energetics of the solvent-coordinated active species require further investigation. We report here a comprehensive computational study of solvent coordination effects on the structure and formation of titanium hydroperoxo complexes using a minimal titanium cluster model. This work focuses on the local interactions between individual solvent molecules and the titanium active site and explores possible ways in which solvent molecules may alter the kinetics and thermodynamics of titanium hydroperoxo intermediate formation. In the second paper of this series, we shall examine the effects of solvent coordination on the reactivity of the titanium hydroperoxo intermediate in the epoxidation of the model olefin ethylene. The overall catalytic cycle for ethylene epoxidation with $Ti(IV)-H_2O_2$ in the presence of solvent coordination at the titanium active site will also be discussed in the next report.

Computational Methodology

All calculations reported here were performed with Gaussian 98[46] and NBO version 5.0[47] software. Density functional theory as implemented in the restricted B3LYP hybrid exchange-correlation scheme was used to include some effects of electron correlation with only a marginal increase in computational cost over Hartree−Fock methods. All results have been obtained for cluster geometries optimized in the gas phase. Solvent continuum effects have been considered for selected cases using the gas-phase optimized geometries in conjunction with the integral equation formalism of the polarizable continuum model (IEF−PCM).[48] All stationary points have been characterized with a full vibrational analysis, and all reported energy differences include zero-point energy corrections. Thermochemistry calculations have been performed at standard temperature and pressure to account for entropy effects associated with ligand coordination. The zero-point energy corrections and thermochemistry results (ΔH, ΔS, and ΔG) have not been scaled. Except where noted, a LANL2DZ effective core potential was used to represent titanium, and a 6-311+G(d,p) basis set was used for all other atoms. Similar computational methods have been shown to yield accurate geometries and energies for similar titanium species.[31,49] Natural bond orbital (NBO) methods were used to analyze the resultant wave functions in terms of optimally chosen, localized orbitals corresponding to a Lewis structure representation of chemical bonding.[50] The occupancies of natural bond orbitals are highly condensed in the most important one-center (lone pair) and two-center (bond) members, allowing electron delocalization effects, or donor−acceptor interactions, to be treated with standard perturbative techniques.

For most calculations, the titanium active site was modeled with unconstrained clusters representing the first coordination sphere of the titanium center. The simplicity of such a cluster model limits the absolute accuracy of the results reported here with regards to real titanium-based epoxidation catalysts. Our computational methodology compromises on model rigor to permit an extremely wide survey of localized solvent coordination effects to be accomplished on a reasonable time scale. This study seeks to elucidate important energetic trends associated with solvent coordination that are relevant to the $Ti(IV)-H_2O_2$ catalytic system in general rather than to describe the absolute energetics applicable to any specific titanium-based catalyst. Any systematic errors arising from the small cluster model should apply to all species and are expected to have a much smaller effect on calculated energy differences. The two chief sources of potential nonsystematic error for this model are the lack of steric constraints and the alterations in the electronic properties of the titanium center and neighboring oxygen atoms caused by cluster truncation. These issues have been addressed for several of the trends reported here using constrained clusters representing the second coordination sphere of the titanium

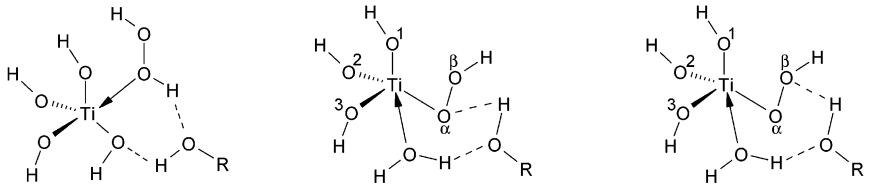

Figure 3. Schematic representation of the hydrogen-bonded bridging interactions between a protic molecule, ROH, and (a) a hydrogen peroxide ligand and a hydroxyl oxygen in a $Ti(OH)_4$ cluster and (b) the proximal or (c) the distal hydroperoxo oxygen and a water ligand in a $Ti(OH)_3(OOH)$ cluster.

active site for a typical support (see details below). Chemical accuracy may be approached by utilizing embedded cluster methods or constrained multiple coordination sphere cluster models to represent the extended environment of the titanium active site. Such calculations will require substantially larger computational resources but could be justified to investigate how particular supports influence the local titanium environment or the general solvent coordination effects described here.

The titanium active site in the absence of solvent coordination was modeled with a $Ti(OH)_4$ cluster. In this cluster, the hydroxyl groups may represent either bonds to framework silicon atoms (Ti−O−Si modeled as Ti−O−H) or hydrolyzed framework linkages. We focus our attention on proton-transfer reactions involving the participation of a single hydroxyl group and treat the other three hydroxyl groups as equivalent, nonreactive structural units. Water, methanol, and hydrogen peroxide molecules were added to the $Ti(OH)_4$ cluster as ligands on titanium. These ligated $Ti(OH)_4$ clusters will be referred to as TiOH−(δH_2O_2, νS) where δ (0 or 1) and ν (0, 1, or 2) are the number of hydrogen peroxide and solvent (S) ligands, respectively, bound to the titanium center. We have also considered the case where a protic molecule coordinates the $Ti(OH)_4$ cluster by simultaneously donating a hydrogen bond to a hydroxyl oxygen atom and receiving a hydrogen bond from a protic solvent or hydrogen peroxide ligand coordinated to titanium (see example in Figure 3a). Clusters with a protic molecule ROH in such a hydrogen-bonded (HB) bridging position will be labeled TiOH−(δH_2O_2, νS, ROH[HB]) using the same nomenclature described above. Larger hydrogen-bonded networks involving multiple protic species are beyond the scope of the present study.

Transition states have been calculated for the formation of titanium hydroperoxo intermediates from the $Ti(OH)_4$ clusters possessing hydrogen peroxide ligands. The optimized transition-state clusters for titanium hydroperoxo intermediate formation will be referred to as TS−TiOH−(δH_2O_2, νS, ROH[HB]) using the reactant nomenclature described above. The existence of a single negative vibrational mode was confirmed for each optimized transition-state structure, and intrinsic reaction coordinate calculations were used to verify the reactants and products corresponding to that mode.[51] Preference is given to the use of the Gibbs free energy of activation over the electronic, or potential, energy of activation as a basis for comparing alternative reaction pathways. The rate constant (k) for an elementary reaction step is defined in terms of the Gibbs activation barrier (ΔG_A) as

$$k = \kappa\left(\frac{k_B T}{h}\right)\exp\left(\frac{-\Delta G_A}{RT}\right) = \kappa\left(\frac{k_B T}{h}\right)\exp\left(\frac{\Delta S_A}{R}\right)\exp\left(\frac{-\Delta H_A}{RT}\right)$$

where κ is the transmission coefficient, k_B is the Boltzmann constant, and ΔS_A and ΔH_A are the entropic and enthalpic activation barriers, respectively. By incorporating entropy effects, the Gibbs activation barrier provides a more complete representation of intrinsic reaction kinetics at nonzero temperatures than the electronic activation barrier.

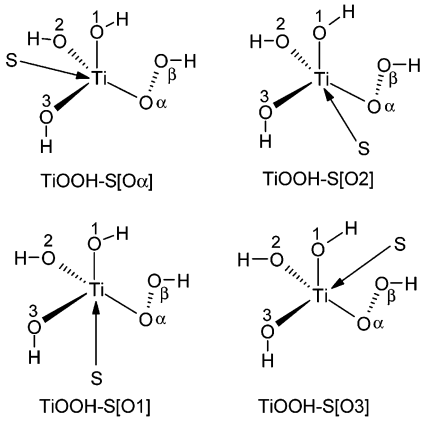

Figure 4. Nomenclature for the orientation of a solvent ligand (S) with respect to the hydroperoxo moiety in a $Ti(OH)_3(OOH)$ complex. The solvent ligand is positioned on the face of the $Ti(OH)_3(OOH)$ tetrahedron opposite the proximal hydroperoxo oxygen Oα or the hydroxyl oxygen O1, O2, or O3. TiOOH−S[O3] is distinguished from TiOOH−S[O1] and TiOOH−S[O2] by having the solvent ligand positioned on the same face of the $Ti(OH)_3(OOH)$ tetrahedron as the distal hydroperoxo oxygen (Oβ).

The resulting titanium hydroperoxo intermediates were modeled with $Ti(OH)_3(OOH)$ clusters. We have numbered the three nonreactive structural hydroxyl groups in $Ti(OH)_3(OOH)$ to help distinguish the four possible orientations of solvent ligands with respect to the hydroperoxo group (see Figure 4). A solvent ligand may coordinate the titanium center in a position trans to the proximal hydroperoxo oxygen Oα or trans to hydroxyl oxygen O1, O2, or O3. We have also optimized $Ti(OH)_3(OOH)$ clusters in which a protic solvent molecule ROH simultaneously receives a hydrogen bond from a ligand on titanium and donates a hydrogen bond to either the proximal (Oα) or distal (Oβ) oxygen of the hydroperoxo group. These hydrogen-bonded bridging positions will be referred to as HB-α and HB-β and are shown schematically in parts b and c of Figure 3. The optimized titanium hydroperoxo clusters will be labeled as TiOOH(η^1 or η^2)−(νS[O#], ROH[HB-α or HB-β]) where η^1 or η^2 denotes monodentate or bidentate hydroperoxo geometry, ν (0, 1, or 2) is the number of solvent ligands coordinating the titanium atom, O# is the label of the oxygen positioned trans to the solvent ligand, and ROH[HB-α or HB-β] indicates the presence of a protic molecule in either of the aforementioned bridging positions. For example, the bidentate $Ti(OH)_3(OOH)$ cluster with two water ligands positioned across from hydroxyl oxygens O1 and O2 and one water molecule in the HB-α bridging position will be abbreviated TiOOH(η^2)−(H_2O[O1], H_2O[O2], H_2O[HB-α]).

To assess utility of the minimal $Ti(OH)_4$ and $Ti(OH)_3(OOH)$ cluster calculations, the second coordination sphere of the titanium active site has been included and modeled with a

TABLE 1: Relative Stabilities of Unconstrained $Ti(OH)_4$ and Constrained $Ti(OSiH_3)_3(OH)$ Complexes[a]

		thermochemistry at 298 K		
	ΔE	ΔH	$T\Delta S$	ΔG
$Ti(OH)_4$ Cluster				
TiOH	0.0	0.0	0.0	0.0
TiOH−H_2O	−5.6	−6.9	−11.2	4.3
TiOH−$2H_2O$	−5.4	−7.2	−20.2	13.0
TiOH−(H_2O, H_2O[HB])	−15.2	−17.5	−21.5	4.0
TiOH−($2H_2O$, H_2O[HB])	−15.3	−18.3	−30.9	12.6
TiOH−MeOH	−6.1	−6.7	−11.9	5.2
TiOH−2MeOH	−8.5	−9.4	−22.8	13.5
TiOH−(MeOH, MeOH[HB])	−16.0	−17.4	−24.2	6.8
TiOH−(2MeOH, MeOH[HB])	−18.3	−19.4	−33.5	14.1
TiOH−H_2O_2	−9.9	−10.8	−12.1	1.3
TiOH−(H_2O_2, H_2O)	−9.1	−11.5	−21.6	10.1
TiOH−(H_2O_2, H_2O[HB])	−18.4	−20.2	−22.1	1.9
TiOH−(H_2O_2, H_2O, H_2O[HB])	−17.7	−20.2	−32.1	11.9
TiOH−(H_2O_2, MeOH)	−9.9	−10.8	−22.6	11.8
TiOH−(H_2O_2, MeOH[HB])	−19.6	−20.7	−22.7	2.0
TiOH−(H_2O_2, H_2O_2[HB])	−19.3	−20.3	−21.9	1.6
$Ti(OSiH_3)_3(OH)$ Cluster				
$Ti(OSiH_3)_3(OH)$	0.0	0.0	0.0	0.0
$Ti(OSiH_3)_3(OH)$−H_2O	−3.1	−4.3	−12.0	7.7
$Ti(OSiH_3)_3(OH)$−H_2O_2	−5.4	−6.2	−13.5	7.3
$Ti(OSiH_3)_3(OH)$−(H_2O_2, H_2O)	−5.9	−7.3	−23.8	16.5
$Ti(OSiH_3)_3(OH)$−(H_2O_2, H_2O[HB])	−13.6	−15.2	−23.7	8.5

[a] Energy changes in kcal/mol calculated relative to the nonligated $Ti(OH)_4$ or $Ti(OSiH_3)_3(OH)$ cluster and coordinating species at infinite separation.

constrained $Ti(OSiH_3)_3(OH)$ cluster in selected cases. This cluster was constructed by substituting a titanium atom for the T-3 silicon atom in the monoclinic MFI framework using the X-ray diffraction coordinates of van Koningsveld et al.[52] A portion of the MFI framework including the titanium atom and its first three coordination spheres was then extracted from the crystal lattice, and hydrogen atoms were added to the dangling bonds of the terminal oxygen atoms along the original bonding direction with the adjacent silicon atoms to yield a $Ti[OSi(OH)_3]_4$ cluster. This cluster was then optimized with the hydrogen atom positions fixed. The first two coordination spheres of the optimized $Ti[OSi(OH)_3]_4$ cluster were then extracted, and hydrogen atoms were added to the dangling bonds of the terminal silicon atoms to yield a $Ti(OSiH_3)_4$ cluster. One siloxyl group on titanium was replaced with a hydroxyl group, and the positions of the remaining silicon atoms were fixed in all subsequent optimizations. The resulting constrained $Ti(OSiH_3)_3(OH)$ cluster was used as the starting point for all calculations involving the second coordination sphere model. These clusters will be labeled as $Ti(OSiH_3)_3(OH)$−(δH_2O_2, νS, ROH[HB]) and $Ti(OSiH_3)_3(OOH)$(η^1 or η^2)−(νS[O#], ROH-[HB-α or HB-β]) using the nomenclature described earlier.

Results and Discussion

Structures and Relative Stabilities of $Ti(OH)_4$ Species. The relative stabilities of several $Ti(OH)_4$ complexes are summarized in Table 1. The addition of a single water, methanol, or hydrogen peroxide ligand to the titanium center is electronically exothermic with $\Delta E = -5.6$, -6.1, or -9.9 kcal/mol, respectively. The entropy loss of binding these ligands increases the Gibbs free energy of the ligated clusters at 298 K by about 11−12 kcal/mol. As a result, the net Gibbs free energy change for the addition of a single water, methanol, or hydrogen peroxide ligand to $Ti(OH)_4$ is endothermic at $\Delta G = 4.3$, 5.2, or 1.3 kcal/mol, respectively. The electronic energy change for addition of a second ligand to titanium is much less exothermic than that of the first ligand, whereas the entropy loss for binding a second ligand to titanium is once again on the order of 10 kcal/mol. Hence, the total ΔG for addition of two ligands exceeds ΔG for addition of a single ligand by over 8 kcal/mol. The presence of a protic molecule (water, methanol, or hydrogen peroxide) in the hydrogen-bonded bridging position confers about 10 kcal/mol of electronic stabilization to the $Ti(OH)_4$ cluster. This electronic stabilization is almost equally offset by the entropy loss arising from the restricted motion of the protic molecule participating in the two hydrogen bonds. The addition of a bridging protic molecule therefore does not significantly alter the relative stability of the $Ti(OH)_4$ complex.

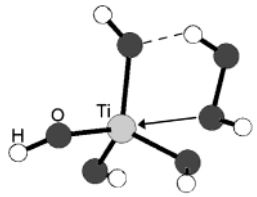

Figure 5. Optimized geometry for TiOH−H_2O_2.

These results indicate that the addition of a single donor ligand to the titanium center in $Ti(OH)_4$ is much more likely than the addition of a second ligand and that protic molecules will readily share two hydrogen bonds with ligated $Ti(OH)_4$ clusters. Both trends are supported by calculations for the constrained $Ti(OSiH_3)_3(OH)$ complexes shown in Table 1. In general, the absolute ligand binding energies for the constrained $Ti(OSiH_3)_3(OH)$ clusters are significantly more endothermic than for the unconstrained $Ti(OH)_4$ clusters.

The addition of a hydrogen peroxide ligand to titanium in the absence of steric constraints is significantly less endothermic than the addition of a water or methanol solvent ligand. Hydrogen peroxide ligands provide increased stabilization because they are capable of simultaneously donating a hydrogen bond to a hydroxyl oxygen while still directly coordinating the titanium center. Figure 5 shows the optimized geometry of the TiOH−H_2O_2 cluster as an example of this hydrogen-bonding motif. The rigid constraints imposed on the larger $Ti(OSiH_3)_3(OH)$−H_2O_2 cluster model hinder optimization of the dual interactions between the hydrogen peroxide ligand and the titanium active site. Because the flexibility of the titanium site in most real Ti(IV)−H_2O_2 catalytic systems is probably intermediate between the two model extremes considered here, it is expected that hydrogen peroxide will compete at least evenly with common donor solvents for adsorption on titanium active sites.

The absolute magnitudes of the electronic energy changes reported in Table 1 agree well with results obtained using other computational methods. Ricchiardi et al.[53] used a combined quantum mechanics-molecular mechanics embedded cluster approach to study the effect of hydration on the structure and location of the titanium active sites in titanium-containing silicalite-1 (TS-1). They found that the electronic binding energies for the addition of one water ligand ranged from −5.5 to −7.4 kcal/mol for three different titanium site locations at the HF/SVP[54] level. The addition of a second water ligand was similarly exothermic for one site ($\Delta E = -7.4$ kcal/mol), endothermic for another site ($\Delta E = 4.8$ kcal/mol), and unstable for the final site. Sinclair et al.[55] studied the addition of one or two water ligands to constrained $Ti(OSiH_3)_4$, $Ti(OSiH_3)_3(OH)$, and $Ti(OSiH_3)_2(OH)_2$ clusters using a BP86/DZVP approach. Their electronic addition energies for the first water ligand ranged between −2.9 and −9.6 kcal/mol, while addition

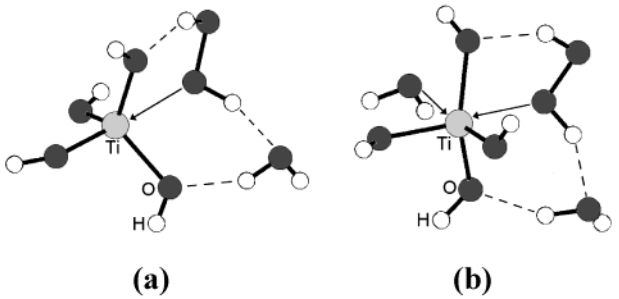

Figure 6. Optimized geometries of representative $Ti(OH)_4$ complexes possessing hydrogen-bonded bridging protic molecules: (a) TiOH−(H_2O_2, H_2O[HB]) and (b) TiOH−(H_2O_2, H_2O, H_2O[HB]).

energies for the second water ligand ranged between −4.1 and −6.9 kcal/mol. Periodic Hartree−Fock calculations of water interaction with a titanium-containing chabazite framework (Si/Ti = 1) performed by Zicovich-Wilson et al.[56] indicated that the total electronic addition energy for one or two water ligands is −8.2 or −10.4 kcal/mol, respectively. The heat of adsorption of water on titanium-containing beta zeolites (Ti-β) has been measured to be 10.3 or 11.9 kcal/mol, depending upon the synthesis method of the catalyst.[6]

The Ti−O bond lengths in the optimized $Ti(OH)_4$ cluster are 1.805−1.806 Å. This result agrees well with EXAFS measurements of Ti═O bond lengths in dehydrated TS-1,[19] Ti-β,[6] and Ti-MCM-41[5] catalysts: 1.793 ± 0.007 Å, 1.80 ± 0.03 Å, and 1.81 ± 0.02 Å, respectively. The distance between the titanium center and the ligand donor atom ranges between 2.22 and 2.47 Å for the cases studied here. These calculated ligand coordination distances are most likely over-estimates because DFT generally has trouble accounting for weak van der Waals forces. Reoptimization of the TiOH−H_2O cluster at the HF and MP2 levels of theory yielded Ti−OH_2 ligand coordination distances of 2.38 and 2.40 Å compared to the B3LYP distance of 2.42 Å. Ricchiardi et al.[53] calculated similar ligand coordination distances for the TiOH−H_2O case. Negligible changes in the optimized geometry of the TiOH−H_2O cluster occur after replacing the ECP on titanium with an all-electron 6-311+G(d,p) basis set. The Ti−O bond distances for hydroxyl oxygen atoms positioned trans to coordinating ligands are approximately 1−7% shorter than the other framework Ti−O bond distances. The ligand donor atom, the titanium center, and the hydroxyl oxygen positioned trans to the donor atom are nearly linear. The angle between these three atoms ranges between 174.3° and 178.7° in the single ligand cases and 159.7° and 176.3° in the double ligand cases. Optimized geometries for the TiOH−(H_2O_2, H_2O[HB]) and TiOH−(H_2O_2, H_2O, H_2O[HB]) clusters are shown in Figure 6 as representative examples of how a protic molecule can simultaneously hydrogen bond to a hydroxyl oxygen and to a hydrogen peroxide ligand.

Formation of Titanium Hydroperoxo Intermediates. We have studied the formation of titanium hydroperoxo intermediates from $Ti(OH)_4$ clusters bearing a single hydrogen peroxide ligand on titanium. The calculated activation energies and reaction energies are summarized in Table 2. We considered two different mechanisms for titanium hydroperoxo intermediate formation, depending upon the absence or presence of a protic molecule in the bridging position. For the TiOH−H_2O_2, TiOH−(H_2O_2, H_2O), and TiOH−(H_2O_2, MeOH) clusters, the hydrogen peroxide ligand transfers a hydrogen from the oxygen coordinating the titanium center to the nearest hydroxyl oxygen. This proton-transfer step results in the transformation of the coordinated hydrogen peroxide ligand into a hydroperoxo group on titanium and the transformation of a hydroxyl group on titanium into a coordinated water ligand. This reaction pathway is illustrated in Figure 7a for the TiOH−H_2O_2 reactant cluster. For the TiOH−(H_2O_2, H_2O[HB]), TiOH−(H_2O_2, MeOH[HB]), TiOH−(H_2O_2, H_2O_2[HB]), and TiOH−(H_2O_2, H_2O, H_2O[HB]) clusters, the hydrogen peroxide ligand transfers a hydrogen from the oxygen coordinating the titanium center to the protic molecule in the bridging position, and the protic molecule simultaneously transfers one of its hydrogens to a hydroxyl oxygen. These two proton-transfer steps occur in a concerted manner through the two pre-existing hydrogen bonds the protic molecule shares with the hydrogen peroxide ligand and the hydroxyl oxygen. This reaction pathway is illustrated in Figure 7b for the TiOH−(H_2O_2, H_2O[HB]) reactant cluster. The net result is the same as the previous case: the transfer of a hydrogen from the hydrogen peroxide ligand to a hydroxyl oxygen and the formation of a hydroperoxo group and water ligand on the titanium center.

The results shown in Table 2 indicate that the addition of a single solvent ligand to the titanium center lowers the Gibbs free energy of activation for titanium hydroperoxo intermediate formation by 4−8.5 kcal/mol. A more complete understanding of this phenomenon requires the NBO analysis developed at the end of this discussion, but a general explanation can be given here. The transfer of the proton from the hydrogen peroxide ligand to the hydroxyl oxygen creates a new water ligand on the titanium center. The octahedral TiOH−(H_2O_2, H_2O) and TiOH−(H_2O_2, MeOH) clusters require significantly less deformation than the pentahedral TiOH−H_2O_2 cluster to accommodate the transformation of a hydroxyl group into a water ligand. As a result, the TS−TiOH−(H_2O_2, H_2O) and TS−TiOH−(H_2O_2, MeOH) transition-state clusters experience a significantly stronger hypervalent donor−acceptor interaction between the developing water ligand and the developing titanium hydroperoxo cluster than the TS−TiOH−H_2O_2 transition-state cluster. The additional stabilization of the TS−TiOH−(H_2O_2, H_2O) and TS−TiOH−(H_2O_2, MeOH) transition states provided

TABLE 2: Activation Barriers and Reaction Energies for the Formation of Titanium Hydroperoxo Intermediates Possessing Various Coordination Environments[a]

	activation barrier		reaction energy[b]	
intermediate formation reaction	ΔE_A	ΔG_A	ΔE_R	ΔG_R
TiOH−H_2O_2 → TiOOH−H_2O	14.9	15.5	2.5	2.3
TiOH−(H_2O_2, H_2O) → TiOOH−2H_2O	9.8	11.4	−1.4	0.5
TiOH−(H_2O_2, MeOH) → TiOOH−(H_2O, MeOH)	6.0	7.0	−2.0	−1.3
TiOH−(H_2O_2, H_2O[HB]) → TiOOH−(H_2O, H_2O[HB-α])	9.5	10.5	1.3	1.2
TiOH−(H_2O_2, MeOH[HB]) → TiOOH−(H_2O, MeOH[HB-α])	8.4	9.5	1.5	1.3
TiOH−(H_2O_2, H_2O_2[HB]) → TiOOH−(H_2O, H_2O_2[HB-α])	8.5	9.7	1.6	1.5
TiOH−(H_2O_2, H_2O, H_2O[HB]) → TiOOH−(2H_2O, H_2O[HB-α])	5.4	6.1	−2.4	−2.1
$Ti(OSiH_3)_3(OH)$−H_2O_2 → $Ti(OSiH_3)_3(OOH)$−H_2O	13.6	12.5	0.7	−0.1
$Ti(OSiH_3)_3(OH)$−(H_2O_2, H_2O[HB]) → $Ti(OSiH_3)_3(OOH)$−(H_2O, H_2O[HB-α])	8.3	8.9	−0.6	−1.7

[a] All energy changes reported in kcal/mol. [b] Reaction energies calculated using representative product species for each reaction (see text).

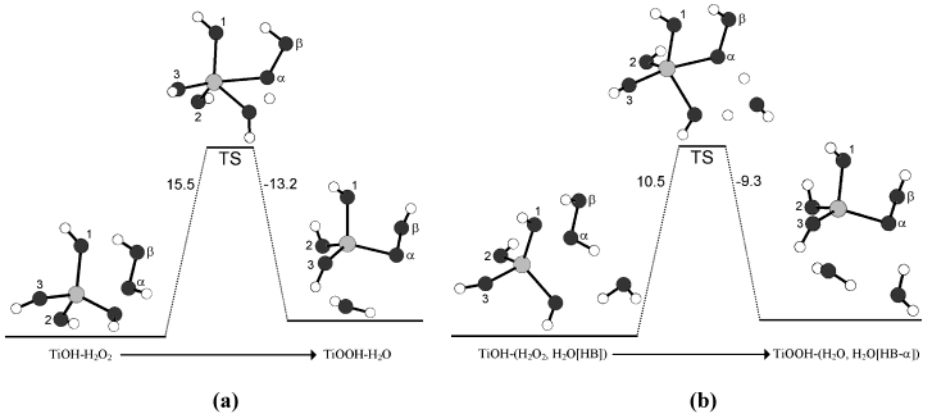

Figure 7. Representative reaction pathways for titanium hydroperoxo intermediate formation in the (a) absence and (b) presence of a hydrogen-bonded bridging protic molecule. The oxygen labeling scheme employed for the titanium hydroperoxo cluster has been extrapolated to the reactant and transition state clusters. Gibbs free energy changes are reported in kcal/mol.

by this donor−acceptor interaction lowers the activation barrier for titanium hydroperoxo intermediate formation.

The presence of a protic molecule in the hydrogen-bonded bridging position lowers the Gibbs free energy of activation for titanium hydroperoxo intermediate formation by about 5−6 kcal/mol. The protic molecule serves as a bridge that facilitates transfer of the hydrogen peroxide proton to a hydroxyl oxygen via the preexisting hydrogen-bond network (as shown in Figure 7b). The decrease in the activation barrier is not surprising if one recognizes that a hydrogen bond essentially represents the partial transfer of a proton. With proton-transfer channels already in place, the structures of the TiOH−(H_2O_2, H_2O[HB]), TiOH−(H_2O_2, MeOH[HB]), and TiOH−(H_2O_2, H_2O_2[HB]) clusters require less deformation than the TiOH−H_2O_2 cluster to accomplish proton transfer from the hydrogen peroxide ligand to the hydroxyl oxygen. As a result, the transition-state occurs earlier, and the activation barrier is lower. A similar effect on activation barriers has been observed previously for other proton-transfer reactions occurring via bridging protic molecules.[57,58] The results for the TiOH−(H_2O_2, H_2O, H_2O[HB]) case indicate that the combined presence of a water ligand on the titanium center and a protic water molecule in the bridging position has a cumulative effect of lowering the Gibbs free energy of activation for titanium hydroperoxo intermediate formation by about 9.5 kcal/mol relative to the TiOH−H_2O_2 case.

The activation barriers calculated for the constrained Ti($OSiH_3$)$_3$(OH)−H_2O_2 and Ti($OSiH_3$)$_3$(OH)−(H_2O_2, H_2O[HB]) clusters are both lower than their Ti(OH)$_4$ counterparts (see Table 2). The difference in ΔG_A between the Ti($OSiH_3$)$_3$(OH)−H_2O_2 and Ti($OSiH_3$)$_3$(OH)−(H_2O_2, H_2O[HB]) clusters is only 3.6 kcal/mol compared to the 5.0 kcal/mol difference calculated for the TiOH−H_2O_2 and TiOH−(H_2O_2, H_2O[HB]) clusters. This discrepancy exists because the rigid atomic constraints increase the relative entropy of the TS−Ti($OSiH_3$)$_3$(OH)−H_2O_2 transition state by preventing a hydrogen-bonding interaction that appears in all of the other transition states for the reactions in Table 2. These results therefore suggest that the degree to which a bridging protic molecule will reduce the Gibbs activation barrier for titanium hydroperoxo intermediate formation in a real Ti(IV)−H_2O_2 catalyst system can depend on the local flexibility of the titanium active site.

The titanium center in an actual titanium-based epoxidation catalyst generally possesses two, three, or four Ti−O−Si bonds to the siliceous framework or support. Hence, proton transfer from a hydrogen peroxide ligand to a framework oxygen may lead to the formation of a silanol group coordinating the titanium center rather than a water ligand. The trends discussed above should be relevant for proton transfer to framework oxygens in both intact Ti−O−Si bonds and hydrolyzed Ti−O−H bonds, although the absolute magnitudes of the energy differences reported in Table 2 are expected to more accurately represent the latter case in real catalysts. To check this hypothesis, we have considered both direct proton transfer from the hydrogen peroxide ligand to the framework siloxyl oxygen in an unconstrained Ti(OH)$_3$($OSiH_3$)·H_2O_2 cluster and bridged proton transfer from the hydrogen peroxide ligand to the framework siloxyl oxygen via the bridging water molecule in an unconstrained Ti(OH)$_3$($OSiH_3$)·(H_2O_2, H_2O[HB]) cluster. The electronic activation barriers (ΔE_A) for Ti(OH)$_3$($OSiH_3$)·H_2O_2 and Ti(OH)$_3$($OSiH_3$)·(H_2O_2, H_2O[HB]) are 17.1 and 11.4 kcal/mol, respectively; the Gibbs activation barriers (ΔG_A) are 18.0 and 13.1 kcal/mol, respectively. The Gibbs activation barriers are both about 2.5 kcal/mol greater than the corresponding barriers for mechanisms in which the hydrogen peroxide proton is transferred to a hydroxyl oxygen. The presence of a protic molecule in the bridging position still lowers the Gibbs activation barrier for titanium hydroperoxo intermediate formation by about 5 kcal/mol.

Because these chemical transformations are typically performed under liquid-phase reaction conditions within the pores of a titanosilicate material, we have estimated the effect of a polarizable reaction medium on the activation barriers. We used the IEF−PCM method with methanol as solvent ($\epsilon = 32.63$) in order to provide a highly polarizable reaction medium. The Gibbs activation barriers for TiOH−H_2O_2 and TiOH−(H_2O_2, H_2O[HB]) in methanol are only slightly reduced by 0.3 and 0.5 kcal/mol, respectively. The Gibbs activation barrier for TiOH−(H_2O_2, H_2O), on the other hand, is moderately increased from 11.4 kcal/mol in the gas phase to 12.9 kcal/mol in a methanol continuum. Thus, the presence of a highly polarizable reaction medium reduces the relative difference between the Gibbs activation barriers for the TiOH−H_2O_2 and TiOH−(H_2O_2, H_2O) cases.

Our results for the formation of the TiOOH−H_2O intermediate from the TiOH−H_2O_2 reactant cluster compare well with the results of previous DFT investigations. Barker et al.[34] calculated two different reaction pathways for proton transfer from a hydrogen peroxide ligand on titanium to a hydroxyl group oxygen in a constrained Ti($OSiH_3$)$_3$(OH) cluster model. The two pathways differed in the initial geometry of the hydrogen peroxide ligand on titanium. They found electronic

TABLE 3: Relative Stabilities[a] and Important Hydroperoxo Group Structural Parameters[b] for Unconstrained $Ti(OH)_3(OOH)$ and Constrained $Ti(OSiH_3)_3(OOH)$ Complexes

		thermochemistry at 298 K			hydroperoxo group geometry		
	ΔE	ΔH	$T\Delta S$	ΔG	D(Oα—Oβ)	D(Ti—Oα)	D(Ti—Oβ)
			$Ti(OH)_3(OOH)$ Cluster				
$TiOOH(\eta^2)$	0.0	0.0	0.0	0.0	1.462	1.873	2.285
$TiOOH(\eta^1)-H_2O$[O1/O2]	−2.9	−3.7	−9.4	5.7	1.433	1.864	2.726
$TiOOH(\eta^2)-H_2O$[O1]	−4.3	−5.3	−10.5	5.2	1.460	1.892	2.380
$TiOOH(\eta^2)-H_2O$[O2]	−2.8	−3.8	−10.0	6.2	1.455	1.894	2.422
$TiOOH(\eta^1)-H_2O$[O3]	−4.0	−5.1	−10.5	5.4	1.442	1.890	2.934
$TiOOH(\eta^2)-(H_2O$[O1], H_2O[O2])	−7.3	−9.7	−21.9	12.2	1.460	1.926	2.382
$TiOOH(\eta^1)-(H_2O$[O1], H_2O[O3])	−6.6	−8.6	−21.3	12.7	1.441	1.935	2.862
$TiOOH(\eta^1)-(H_2O$[Oα], H_2O[O1])	−5.9	−7.9	−20.8	12.9	1.429	1.860	2.877
$TiOOH(\eta^1)-(H_2O$[Oα], H_2O[O2])	−5.8	−7.7	−20.2	12.6	1.426	1.834	2.844
$TiOOH(\eta^2)-$(MeOH[O1], H_2O[O2])	−8.8	−10.2	−22.3	12.1	1.450	1.934	2.412
$TiOOH(\eta^2)-(H_2O$[O1], H_2O[HB-α])	−14.0	−16.0	−20.7	4.6	1.458	1.918	2.432
$TiOOH(\eta^2)-(H_2O$[O1], H_2O[HB-β])	−12.2	−13.7	−19.3	5.6	1.465	1.912	2.451
$TiOOH(\eta^2)-$(MeOH[HB-α])	−14.9	−16.3	−21.2	4.9	1.458	1.918	2.434
$TiOOH(\eta^2)-(H_2O$[O1], H_2O_2[HB-α])	−14.6	−15.8	−20.4	4.6	1.458	1.921	2.451
$TiOOH(\eta^2)-(H_2O$[O1], H_2O[O2], H_2O[HB-α])	−16.8	−19.5	−30.8	11.3	1.452	1.956	2.432
			$Ti(OSiH_3)_3(OOH)$ Cluster				
$Ti(OSiH_3)_3(OOH)$	0.0	0.0	0.0	0.0	1.465	1.878	2.292
$Ti(OSiH_3)_3(OOH)(\eta^1)-H_2O$[O1/O2]	−1.8	−2.4	−10.0	7.6	1.432	1.877	2.907
$Ti(OSiH_3)_3(OOH)(\eta^2)-H_2O$[O1]	−3.1	−3.7	−10.2	6.5	1.468	1.921	2.292
$Ti(OSiH_3)_3(OOH)(\eta^1)-H_2O$[O3]	−3.0	−3.7	−10.1	6.4	1.444	1.904	2.954
$Ti(OSiH_3)_3(OOH)$ $(\eta^2)-(H_2O$[O1],H_2O[HB-α])	−12.5	−14.0	−20.1	6.1	1.466	1.951	2.291

[a] Energy changes in kcal/mol calculated relative to the nonligated $Ti(OH)_3(OOH)$ and $Ti(OSiH_3)_3(OOH)$ clusters and coordinating species at infinite separation. [b] Bond distances in Å.

activation barriers of 9.1 and 11.0 kcal/mol for the two pathways using a BP86/DZVP approach. In the present study, only one optimized geometry for hydrogen peroxide adsorbed on the bare $Ti(OH)_4$ cluster has been obtained (Figure 5), and the electronic activation barrier for proton transfer in that cluster is 14.9 kcal/mol. It is generally found that pure density functionals, such as BP86, tend to yield lower activation barriers than hybrid density functionals, such as B3LYP, because hybrid functionals partially account for exact exchange.[59,60] Reoptimization of our $TiOH-H_2O_2$ and $TS-TiOH-H_2O_2$ clusters using BP86 with the original basis set yields an activation barrier of 10.7 kcal/mol, in close agreement with the results of Barker et al.[34] The use of an effective core potential to model titanium has little effect on the activation barrier. The electronic activation barrier for formation of $TiOOH-H_2O$ becomes 14.5 kcal/mol upon reoptimization with an all electron B3LYP/6-311+G(d,p) methodology. Munakata et al.[45] calculated an electronic activation barrier of 16.5 kcal/mol for the transfer of a proton from a hydrogen peroxide ligand on titanium to a framework oxygen in a constrained $Ti[OSi(OH)_3]_4$ cluster model. In their case, proton-transfer yields a silanol coordinated to the titanium center instead of a water ligand. The electronic activation barrier for the same process in our unconstrained $Ti(OH)_3(OSiH_3)\cdot H_2O_2$ cluster is similar at 17.1 kcal/mol. Munakata et al.[45] proposed that the resulting titanium hydroperoxo intermediate rearranges to form a TiOOSi species with an activation barrier of 13.9 kcal/mol. No reports of titanium hydroperoxo intermediate formation with reactant complexes possessing solvent ligands on titanium or bridging protic molecules are available for comparison.

Structures and Relative Stabilities of $Ti(OH)_3(OOH)$ Intermediates. The transformation of a hydrogen peroxide ligand on titanium into a hydroperoxo group concomitantly generates a new water ligand on titanium (or silanol ligand if proton transfer to a Ti−O−Si linkage is considered). This water ligand will be positioned trans to hydroxyl oxygen O1 or O2 (see Figure 4). The relative stabilities and bond distances of these optimized titanium hydroperoxo intermediates are summarized in Table 3. Stable geometries have been found for both monodentate (η^1) and bidentate (η^2) coordination of the hydroperoxo moiety in the $TiOOH-H_2O$[O1] and $TiOOH-H_2O$[O2] clusters. The optimized monodentate structures of $TiOOH-H_2O$[O1] and $TiOOH-H_2O$[O2] are equivalent and will be labeled as $TiOOH(\eta^1)-H_2O$[O1/O2]. In this case, monodentate coordination is stabilized by the presence of a hydrogen bond between the hydroperoxo group and a hydroxyl oxygen as shown in the optimized structure in Figure 8a. This hydrogen-bonding channel exists in the $TiOH-H_2O_2$ reactant (Figure 5) and the $TS-TiOH-H_2O_2$ transition state and persists into the $TiOOH(\eta^1)-H_2O$[O1/O2] product. In the absence of this hydrogen-bonding interaction, the hydroperoxo moiety assumes bidentate coordination to the titanium center. The optimized structures of the bidentate titanium hydroperoxo intermediates, $TiOOH(\eta^2)-H_2O$[O1] and $TiOOH(\eta^2)-H_2O$[O2], are shown in parts b and c of Figure 8. The relative stabilities of $TiOOH(\eta^1)-H_2O$[O1/O2], $TiOOH(\eta^2)-H_2O$[O1], and $TiOOH(\eta^2)-H_2O$[O2] are similar with ligand binding free energies of 5.7, 5.2, and 6.2 kcal/mol, respectively. Thus, the stabilization obtained through coordination of the distal hydroperoxo oxygen at the titanium center is similar to the stabilization conferred through the hydrogen bond between the hydroperoxo hydrogen and the hydroxyl oxygen. Optimization of the $Ti(OH)_3(OOH)$ cluster in the absence of ligands on titanium invariably yields a bidentate hydroperoxo group.

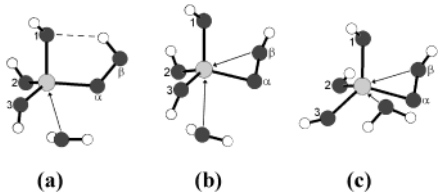

Figure 8. Optimized geometries for mono-ligated titanium hydroperoxo intermediates: (a) $TiOOH(\eta^1)-H_2O$[O1/O2], (b) $TiOOH(\eta^2)-H_2O$[O1], and (c) $TiOOH(\eta^2)-H_2O$[O2].

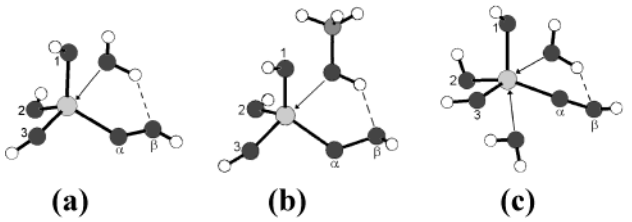

Figure 9. Optimized geometries for hydrogen-bonded five-membered ring titanium hydroperoxo intermediates: (a) TiOOH(η^1)−H_2O[O3], (b) TiOOH(η^1)−MeOH[O3], and (c) TiOOH(η^1)−(H_2O[O1], H_2O[O3]).

The hydroperoxo moiety in the various TiOOH−H_2O clusters may reorient to yield TiOOH(η^1)−H_2O[O3]. In this case, the hydroperoxo group is stabilized in monodentate coordination with the titanium center via a hydrogen bond between the water ligand and the distal oxygen of the hydroperoxo group. The optimized geometry for TiOOH(η^1)−H_2O[O3] is shown in Figure 9a. This structure resembles the hydrogen-bonded five-membered ring titanium hydroperoxo species proposed by Clerici and co-workers[25,26] (Figure 2) as the active oxygen-donating intermediate in epoxidation reactions with titanium-containing molecular sieves. This monodentate five-membered ring structure can also form with other protic solvents as shown for the case of TiOOH(η^1)−MeOH[O3] in Figure 9b. It should be noted that the hydrogen-bonding motif observed in the structure of TiOOH(η^1)−H_2O[O1/O2] (Figure 8a) also constitutes a five-membered ring. To avoid ambiguous nomenclature, only the cyclic hydrogen-bonding motif proposed by Clerici and co-workers where the coordinated solvent ligand directly participates in the ring will be referred to as the "five-membered ring intermediate" in the remainder of this discussion. The results given in Table 3 show that no significant additional stabilization is obtained by the formation of a five-membered ring structure via hydrogen bonding with a protic ligand. The formation of the five-membered ring TiOOH(η^1)−H_2O[O3] intermediate is therefore as equally probable as formation of the other TiOOH−H_2O intermediates. This conclusion agrees with the recently reported results of Barker et al.,[34,35] who showed that a bidentate $Ti(OSiH_3)_3(OOH)\cdot H_2O$ cluster is only 0.6 kcal/mol more stable than a monodentate five-membered ring $Ti(OSiH_3)_3(OOH)\cdot H_2O$ cluster.

Depending upon the coordination environment of the $Ti(OH)_4$ precursor species, the titanium hydroperoxo intermediate may be formed with a second ligand on titanium or a protic molecule in the hydrogen-bonded bridging position (see reactions in Table 2). Titanium hydroperoxo complexes formed with a single water ligand on titanium may also add a second solvent ligand on titanium or a protic molecule in the bridging position after the formation reaction is completed. In the absence of steric effects caused by the titanium environment, a second ligand can add to the titanium center at any of the positions shown in Figure 4. It is expected, however, that steric effects in real titanium-based epoxidation catalysts will ultimately make certain ligand orientations preferable. Representative cases have been considered for all possibilities; the results are presented in Table 3.

The relative stabilities of the $Ti(OH)_3(OOH)$ clusters presented in Table 3 follow trends similar to those seen for the $Ti(OH)_4$ clusters in Table 1. The addition of a single water ligand to the $Ti(OH)_3(OOH)$ cluster is electronically exothermic with a ligand binding energy between −2.8 and −4.3 kcal/mol. Binding a ligand to the titanium center once again produces an entropy loss of about 10 kcal/mol at 298 K, and as a result, the Gibbs free energy change for addition of a single water ligand is about 5−6 kcal/mol. The electronic energy change for addition of a second ligand to a TiOOH−H_2O cluster is slightly exothermic. The entropy loss, however, once again dominates the small enthalpic term, and ΔG for addition of a second ligand to a TiOOH−H_2O cluster is about 6−7 kcal/mol. Thus, it is unlikely that titanium hydroperoxo intermediates formed with a single water ligand on titanium will add a second ligand. The presence of a protic molecule at the HB-α bridging position (see nomenclature in Figure 3) provides an additional electronic stabilization of about 10 kcal/mol. This stabilization is almost equally offset by the concomitant entropy loss, and as a result, ΔG changes little upon addition of a protic molecule at the HB-α position. Comparison of results for the TiOOH−(H_2O[O1], H_2O[HB-α]) and TiOOH−(H_2O[O1], H_2O[HB-β]) clusters indicates that little energetic preference exists for the HB-α bridging position compared to the HB-β bridging position. Hence, protic molecules will readily complex ligated titanium hydroperoxo intermediates at both hydrogen-bonded bridging sites.

The hydroperoxo groups in the TiOOH(η^2)−(H_2O[O1], H_2O[O2]) and TiOOH(η^2)−(MeOH[O1], H_2O[O2]) clusters are coordinated in a bidentate manner to the titanium center, giving titanium a first sphere coordination number close to seven. The hydroperoxo group is monodentate, however, when two water ligands coordinate the titanium center with one positioned across from the proximal hydroperoxo oxygen Oα. In these cases, monodentate coordination is stabilized in a manner similar to TiOOH(η^1)−H_2O[O1/O2] by the presence of a hydrogen bond between the hydroperoxo group and a hydroxyl oxygen. As with the single ligand TiOOH(η^1)−H_2O[O3] or TiOOH(η^1)−MeOH[O3] cases described above, the hydroperoxo moiety in doubly ligated $Ti(OH)_3(OOH)$ complexes can also be stabilized in monodentate coordination via hydrogen bonding in a five-membered ring structure with a protic ligand on titanium. The optimized geometry of the TiOOH(η^1)−(H_2O[O1], H_2O[O3]) cluster is shown in Figure 9c. These results demonstrate that the orientation of the ligands around the titanium center controls the optimized geometry of the hydroperoxo moiety in doubly ligated $Ti(OH)_3(OOH)$ clusters. Previous studies of doubly ligated titanium hydroperoxo intermediates have not considered multiple ligand orientations, and as a result, only the possible existence of the monodentate five-membered ring intermediate has been reported.[28,34] The present study indicates that bidentate coordination and other mechanisms of monodentate coordination are also possible. The TiOOH−(H_2O[O1], ROH[HB-α or HB-β]) clusters all have bidentate hydroperoxo moieties. Adding a second water ligand to TiOOH(η^2)−(H_2O[O1], H_2O[HB-α]) in a position trans to hydroxyl oxygen O2 does not change the bidentate coordination of the hydroperoxo group. The framework Ti−O bond lengths and the coordination angles of the solvent ligands for the $Ti(OH)_3(OOH)$ complexes follow trends similar to the ones discussed above for the $Ti(OH)_4$ complexes.

The results of calculations on the larger, constrained $Ti(OSiH_3)_3(OOH)$ clusters support several of the trends described above. The relative stabilities of the $Ti(OSiH_3)_3(OOH)$(η^1)−H_2O[O1/O2], $Ti(OSiH_3)_3(OOH)$(η^2)−H_2O[O1], $Ti(OSiH_3)_3(OOH)$(η^1)−H_2O[O3], and $Ti(OSiH_3)_3(OOH)$(η^2)−(H_2O[O1], H_2O[HB-α]) clusters are all similar. The geometry of the hydroperoxo moiety also changes little as a result of using the larger cluster models.

NBO Analysis of Ligand Coordination. NBO analysis reveals that the primary donor−acceptor interaction arising from solvent ligand coordination at the $Ti(OH)_4$ and $Ti(OH)_3(OOH)$ clusters is a donation from a lone pair on the solvent ligand to the σ_{Ti-O}* antibonding orbital positioned directly across from

it. For example, when a single water ligand is coordinated to the titanium center trans to the proximal hydroperoxo oxygen Oα, one of its lone pairs donates electrons into the $\sigma_{Ti-O\alpha}$* antibonding orbital. This pattern of $n_S \rightarrow \sigma_{Ti-O}$* delocalization is a common feature of transition metal coordination complexes.[61] It indicates the existence of a near-linear 3-center, 4-electron hypervalent ω bond between the solvent ligand, the titanium center, and the oxygen atom directly across from the ligand. Second-order perturbation theory estimates of the stabilization energies accompanying these hypervalent donor−acceptor interactions range between 35 and 65 kcal/mol for ligands on $Ti(OH)_4$ and 25 and 55 kcal/mol for ligands on $Ti(OH)_3(OOH)$. In each case, the $n_S \rightarrow \sigma_{Ti-O}$* delocalization is quite strong and leads to a significant transfer of about 0.06 to 0.13 electrons from the ligand to the titanium hydroperoxo cluster. The σ_{Ti-O}* antibond orbital participating in the ω bond generally polarizes slightly toward oxygen in order to improve backside interaction with the donor ligand lone pair. Conversely, the σ_{Ti-O} bond orbital generally polarizes toward titanium. The titanium hybridization also changes systematically to accommodate formation of the ω bond, with the titanium hybrids in σ_{Ti-O} bonds possessing approximately sd^{4-7} hybridization and the titanium hybrids in ω_{Ti-O} bonds possessing approximately sd^2 hybridization.

NBO analysis helps elucidate the effect of an additional solvent ligand on the activation barrier for titanium hydroperoxo intermediate formation. Examination of the primary donor−acceptor interactions for the near-octahedral TS−TiOH−(H_2O_2, H_2O) and TS−TiOH−(H_2O_2, MeOH) transition-state clusters indicates the existence of an ω bond between the developing water ligand and the σ_{Ti-O}* antibond orbital positioned most nearly trans to it. The strength of this ω-bond interaction is about 59 kcal/mol for the TS−TiOH−(H_2O_2, H_2O) case and 40 kcal/mol for the TS−TiOH−(H_2O_2, MeOH) case. The strongest donor−acceptor interaction between the developing water ligand and a framework σ_{Ti-O}* antibond orbital in the TS−TiOH−H_2O_2 cluster is only about 9 kcal/mol. Other electronic and structural modifications associated with solvent coordination certainly play a role in determining the actual calculated differences in activation barriers for these three cases, but the presence or absence of this ω-bond interaction in the transition state is the most salient difference among the clusters considered and likely controls the observed reactivity.

The principal donor−acceptor interaction stabilizing the bidentate coordination of the distal hydroperoxo oxygen Oβ is a donation from the lone pair of Oβ into the antibonding orbital between titanium and hydroxyl oxygen O3 ($n_{O\beta} \rightarrow \sigma_{Ti-O3}$*). The strength of this donation for the $Ti(OH)_3(OOH)$ clusters ranges between 17 and 30 kcal/mol, and it results in a transfer of about 0.04−0.08 electrons. This interaction essentially represents the existence of another weak 3-center, 4-electron hypervalent ω bond between the distal hydroperoxo oxygen Oβ, the titanium center, and hydroxyl oxygen O3. The $n_{O\beta} \rightarrow \sigma_{Ti-O3}$* interaction is absent for all of the monodentate titanium hydroperoxo clusters examined in this study. In those cases, NBO analysis verifies the existence of the $n_O \rightarrow \sigma_{O-H}$* hydrogen-bond interactions that stabilize monodentate coordination of the hydroperoxo group.

Conclusions

Titanium hydroperoxo intermediates can be formed with a variety of coordination environments under liquid-phase reaction conditions. In the absence of hydrogen-bonded bridging protic molecules, the lowest activation barrier for titanium hydroperoxo intermediate formation occurs when the titanium center possesses a second donor ligand in addition to adsorbed hydrogen peroxide. The addition of a second ligand to the titanium center is thermodynamically unfavorable, however. Comparison of the relative stabilities and activation barriers for singly and doubly ligated $Ti(OH)_4$ complexes indicates that the predominant intermediate formation pathway will occur through titanium sites possessing only a single hydrogen peroxide ligand. The most abundant titanium hydroperoxo intermediate formed in the absence of bridging protic molecules therefore will be the TiOOH−H_2O species. A multiplicity of degenerate TiOOH−H_2O structures exist, some with bidentate and others with monodentate coordination of the hydroperoxo moiety. It has been shown that monodentate coordination can be stabilized either by a hydrogen bond between the distal oxygen of the hydroperoxo group and a protic ligand on titanium or by a hydrogen bond between the hydrogen of the hydroperoxo group and a hydroxyl oxygen.

Unlike the coordination of a second ligand to the titanium center, the addition of a protic molecule to the hydrogen-bonded bridging position is thermodynamically favorable. A bridging protic molecule facilitates proton transfer from the hydrogen peroxide ligand and lowers the activation barrier for titanium hydroperoxo intermediate formation by about 5−6 kcal/mol. The thermodynamic and kinetic evidence therefore suggests that this bridging reaction pathway should make a significant contribution to the production of the titanium hydroperoxo intermediate and may, in fact, take precedence as the primary pathway for intermediate formation, especially in protic solvents. The existence of this pathway may help explain the experimentally observed beneficial effect of protic solvents on epoxidation reaction rates with hydrophobic titanium-based catalysts. This reaction pathway is viable even in aprotic solvents because protic species are introduced through the use of aqueous hydrogen peroxide as the oxidant. It is therefore expected that TiOOH−(H_2O, ROH[HB-α or HB-β]) species will be abundant titanium hydroperoxo intermediates.

These theoretical predictions agree well with the recent experimental results of Sankar et al.,[33] who characterized the local geometry of titanium active sites in Ti-grafted MCM-41 catalysts after reaction with *t*-butyl hydroperoxide using in situ X-ray absorption spectroscopy and found that the titanium center most likely possesses octahedral coordination consistent with the possible existence of a bidentate hydroperoxo moiety and a single water ligand on titanium. The most abundant titanium hydroperoxo intermediates predicted by our computational study, TiOOH−H_2O and TiOOH−(H_2O, ROH[HB-α or HB-β]), can possess the same local coordination environment.

The present study shows that hydrogen bonding with a protic solvent molecule in a five-membered ring does not confer significant additional stabilization to the TiOOH−H_2O intermediate. Thus, the five-membered ring intermediate cannot be invoked on this basis as an explanation for epoxidation rate enhancement in protic solvents. The five-membered ring intermediate may, however, be more reactive toward olefins than other TiOOH−H_2O intermediates. The next paper in this series will clarify the effects of solvent coordination on the reactivity of titanium hydroperoxo complexes in the epoxidation of the model olefin ethylene. The overall catalytic cycle for ethylene epoxidation with Ti(IV)−H_2O_2 in the presence of solvent coordination at the titanium active site will also be discussed in the next report.

Acknowledgment. We gratefully acknowledge the financial support of the National Science Foundation Training Grant

(DGE−9554586) for the program "Catalysis for Environmentally Conscious Manufacturing" and funding received through a National Science Foundation Fellowship (R.R.S.). We also thank Dr. Frank A. Weinhold for helpful discussions.

References and Notes

(1) Dutoit, D. C. M.; Schneider, M.; Baiker, A. *J. Catal.* **1995**, *153*, 165−176.
(2) Klein, S.; Thorimbert, S.; Maier, W. F. *J. Catal.* **1996**, *163*, 476−488.
(3) Kochkar, H.; Figueras, F. *J. Catal.* **1997**, *171*, 420−430.
(4) Taramasso, M.; Perego, G.; Notari, B., U. S. Patent, 4,410,501, 1983.
(5) Blasco, T.; Corma, A.; Navarro, M. T.; Pariente, J. P. *J. Catal.* **1995**, *156*, 65−74.
(6) Blasco, T.; Camblor, M. A.; Corma, A.; Esteve, P.; Guil, J. M.; Martínez, A.; Perdigón-Melón, J. A.; Valencia, S. *J. Phys. Chem. B* **1998**, *102*, 75−88.
(7) Wulff, H. P., British Patent, 1,249,079, 1971.
(8) Jorda, E.; Tuel, A.; Teissier, R.; Kervennal, J. *J. Catal.* **1998**, *175*, 93−107.
(9) Holmes, S. A.; Quignard, F.; Choplin, A.; Teissier, R.; Kervennal, J. *J. Catal.* **1998**, *176*, 173−181.
(10) Fraile, J. M.; García, J. I.; Mayoral, J. A.; Vispe, E. *J. Catal.* **2000**, *189*, 40−51.
(11) Maschmeyer, T.; Rey, F.; Sankar, G.; Thomas, J. M. *Nature* **1995**, *378*, 159−162.
(12) Krijnen, S.; Mojet, B. L.; Abbenhuis, H. C. L.; Van Hooff, J. H. C.; Van Santen, R. A. *Phys. Chem. Chem. Phys.* **1999**, *1*, 361−365.
(13) Corma, A.; Fornes, V.; Pergher, S. B.; Maesen, Th. L. M.; Buglass, J. G. *Nature* **1998**, *396*, 353−356.
(14) Hutter, R.; Mallat, T.; Baiker, A. *J. Catal.* **1995**, *153*, 177−189.
(15) Notari, B. *Adv. Catal.* **1996**, *41*, 253−334.
(16) Alba, M. D.; Luan, Z.; Klinowski, J. *J. Phys. Chem.* **1996**, *100*, 2178−82.
(17) Prakash, A. M.; Sung-Suh, H. M.; Kevan, L. *J. Phys. Chem. B* **1998**, *102*, 857−864.
(18) Marchese, L.; Maschmeyer, T.; Gianotti, E.; Coluccia, S.; Thomas, J. M. *J. Phys. Chem. B* **1997**, *101*, 8836−8838.
(19) Lamberti, C.; Bordiga, S.; Arduino, D.; Zecchina, A.; Geobaldo, F.; Spanó, G.; Genoni, F.; Petrini, G.; Carati, A.; Villain, F.; Vlaic, G. *J. Phys. Chem. B* **1998**, *102*, 6382−6390.
(20) Le Noc, L.; On, D. T.; Solomykina, S.; Echchahed, B.; Béland, F.; dit Moulin, C. C.; Bonneviot, L. *Stud. Surf. Sci. Catal.* **1996**, *101*, 611−620.
(21) Corma, A.; García, H.; Navarro, M. T.; Palomares, E. J.; Rey, F. *Chem. Mater.* **2000**, *12*, 3068−3072.
(22) Sinclair, P. E.; Catlow, C. R. A. *Chem. Commun.* **1997**, 1881−1882.
(23) Boccuti, M. R.; Zecchina, A.; Leofanti, G.; Petrini, G. *Stud. Surf. Sci. Catal.* **1989**, *48*, 133−144.
(24) Marchese, L.; Gianotti, E.; Dellarocca, V.; Maschmeyer, T.; Rey, F.; Coluccia, S.; Thomas, J. M. *Phys. Chem. Chem. Phys.* **1999**, *1*, 585−592.
(25) Bellussi, G.; Carati, A.; Clerici, M. G.; Maddinelli, G.; Millini, R. *J. Catal.* **1992**, *133*, 220−230.
(26) Clerici, M. G.; Ingallina, P. *J. Catal.* **1993**, *140*, 71−83.
(27) Zecchina, A.; Bordiga, S.; Lamberti, C.; Ricchiardi, G.; Scarano, D.; Petrini, G.; Leofanti, G.; Mantegazza, M. *Catal. Today* **1996**, *32*, 97−106.
(28) Tozzola, G.; Mantegazza, M. A.; Ranghino, G.; Petrini, G.; Bordiga, S.; Ricchiardi, G.; Lamberti, C.; Zulian, R.; Zecchina, A. *J. Catal.* **1998**, *179*, 64−71.
(29) Lin, W.; Frei, H. *J. Am. Chem. Soc.* **2002**, *124*, 9292−9298.
(30) Karlsen, E.; Schöffel, K. *Catal. Today* **1996**, *32*, 107−114.
(31) Yudanov, I. V.; Gisdakis, P.; Valentin, C. D.; Rösch, N. *Eur. J. Inorg. Chem.* **1999**, 2135−2145.
(32) Sinclair, P. E.; Catlow, C. R. A. *J. Phys. Chem. B* **1999**, *103*, 1084−1095.
(33) Sankar, G.; Thomas, J. M.; Catlow, C. R. A.; Barker, C. M.; Gleeson, D.; Kaltsoyannis, N. *J. Phys. Chem. B* **2001**, *105*, 9028−9030.
(34) Barker, C. M.; Kaltsoyannis, N.; Catlow, C. R. A. *Stud. Surf. Sci. Catal.* **2001**, *135*, 2580−2587.
(35) Barker, C. M.; Gleeson, D.; Kaltsoyannis, N.; Catlow, C. R. A.; Sankar, G.; Thomas, J. M. *Phys. Chem. Chem. Phys.* **2002**, *4*, 1228−1240.
(36) Clerici, M. G.; Bellussi, G.; Romano, U. *J. Catal.* **1991**, *129*, 159−167.
(37) Sato, T.; Dakka, J.; Sheldon, R. A. *Stud. Surf. Sci. Catal.* **1994**, *84*, 1853−1860.
(38) Van der Waal, J. C.; van Bekkum, H. *J. Mol. Catal. A* **1997**, *124*, 137−146.
(39) Hulea, V.; Dumitriu, E.; Patcas, F.; Ropot, R.; Graffin, P.; Moreau, P. *Appl. Catal. A* **1998**, *170*, 169−175.
(40) Langhendries, G.; De Vos, D. E.; Baron, G. V.; Jacobs, P. A. *J. Catal.* **1999**, *187*, 453−463.
(41) Ingold, K. U.; Snelgrove, D. W.; MacFaul, P. A.; Oldroyd, R. D.; Thomas, J. M. *Catal. Lett.* **1997**, *48*, 21−24.
(42) Müller, C. A.; Deck, R.; Mallat, T.; Baiker, A. *Top. Catal.* **2000**, *11/12*, 369−378.
(43) Vayssilov, G. N.; van Santen, R. A. *J. Catal.* **1998**, *175*, 170−174.
(44) Tantanak, D.; Vincent, M. A.; Hillier, I. H. *Chem. Commun.* **1998**, 1031−1032.
(45) Munakata, H.; Oumi, Y.; Miyamoto, A. *J. Phys. Chem. B* **2001**, *105*, 3493−3501.
(46) Frisch, M. J.; Trucks, G. W.; Schlegel, H. B.; Scuseria, G. E.; Robb, M. A.; Cheeseman, J. R.; Zakrzewski, V. G.; Montgomery, J. A., Jr.; Stratmann, R. E.; Burant, J. C.; Dapprich, S.; Millam, J. M.; Daniels, A. D.; Kudin, K. N.; Strain, M. C.; Farkas, O.; Tomasi, J.; Barone, V.; Cossi, M.; Cammi, R.; Mennucci, B.; Pomelli, C.; Adamo, C.; Clifford, S.; Ochterski, J.; Petersson, G. A.; Ayala, P. Y.; Cui, Q.; Morokuma, K.; Malick, D. K.; Rabuck, A. D.; Raghavachari, K.; Foresman, J. B.; Cioslowski, J.; Ortiz, J. V.; Stefanov, B. B.; Liu, G.; Liashenko, A.; Piskorz, P.; Komaromi, I.; Gomperts, R.; Martin, R. L.; Fox, D. J.; Keith, T.; Al-Laham, M. A.; Peng, C. Y.; Nanayakkara, A.; Gonzalez, C.; Challacombe, M.; Gill, P. M. W.; Johnson, B. G.; Chen, W.; Wong, M. W.; Andres, J. L.; Head-Gordon, M.; Replogle, E. S.; Pople, J. A. *Gaussian 98*, revision A.9; Gaussian, Inc., Pittsburgh, PA, 1998.
(47) NBO 5.0. Glendening, E. D.; Badenhoop, J. K.; Reed, A. E.; Carpenter, J. E.; Bohmann, J. A.; Morales, C. M.; Weinhold, F. Theoretical Chemistry Institute, University of Wisconsin: Madison, WI, 2001.
(48) Cancès, E.; Mennucci, B.; Tomasi, J. *J. Chem. Phys.* **1997**, *107*, 3032−3041.
(49) Sastre, G.; Corma, A. *Chem. Phys. Lett.* **1999**, *302*, 447−453.
(50) Weinhold, F. A. *Encyclopedia of Computational Chemistry*; John Wiley & Sons: New York, 1998.
(51) Gonzalez, C.; Schlegel, H. B. *J. Chem. Phys.* **1989**, *90*, 2154−2161.
(52) van Koningsveld, H.; Jansen, J. C.; van Bekkum, H. *Zeolites* **1990**, *10*, 235−242.
(53) Ricchiardi, G.; de Man, A.; Sauer, J. *Phys. Chem. Chem. Phys.* **2000**, *2*, 2195−2204.
(54) Schäfer, A.; Horn, H.; Ahlrichs, R. *J. Chem. Phys.* **1992**, *97*, 2571−2577.
(55) Sinclair, P. E.; Sankar, G.; Catlow, C. R. A.; Thomas, J. M.; Maschmeyer, T. *J. Phys. Chem. B* **1997**, *101*, 4232−4237.
(56) Zicovich-Wilson, C. M.; Dovesi, R.; Corma, A. *J. Phys. Chem. B* **1999**, *103*, 988−994.
(57) Nguyen, K. A.; Gordon, M. S.; Truhlar, D. G. *J. Am. Chem. Soc.* **1991**, *113*, 1596−1600.
(58) Okuno, Y. *Chem. Eur. J.* **1997**, *3*, 212−218.
(59) Deubel, D. V. *J. Phys. Chem. A* **2001**, *105*, 4765−4772.
(60) Durant, J. L. *Computational Thermochemistry: Prediction and Estimation of Molecular Thermodynamics*. American Chemical Society: Washington, DC, 1998.
(61) Weinhold, F.; Landis, C. R. *Valency and Bonding: A Natural Bond Orbital Donor−Acceptor Perspective.* (in preparation).